A.Ye. Ayazbayeva[1, 2*], S.Z. Nauryzova[2], V.O. Aseyev[3], A.V. Shakhvorostov[1]

[1]Institute of Polymer Materials and Technology, Almaty, Kazakhstan;
[2]Satbayev University, Almaty, Kazakhstan;
[3]Department of Chemistry, University of Helsinki, Helsinki, Finland
(*Corresponding author's e-mail: ayazbayeva.aigerim@gmail.com)

Immobilization of Methyl Orange and Methylene Blue within the Matrix of Charge-Imbalanced Amphoteric Nanogels and Study of Dye Release Kinetics as a Function of Temperature and Ionic Strength

Cross-linked polyampholyte nanogels consisting of neutral N-isopropylacrylamide (NIPAM), negatively charged sodium salt of 2-acrylamido-2-methylpropanesulfonate (AMPS), and positively charged (3-acryl-amidopropyltrimethylammonium chloride (APTAC) monomers were synthesized via conventional redox initiated free radical copolymerization using N,N-methylenebis(acrylamide) (MBAA) as a crosslinking agent. The resulting nanogels were characterized by means of FTIR and ^{1}H NMR spectroscopy, dynamic light scattering (DLS) and zeta-potential measurements. Surface morphology was analyzed using scanning electron microscopy. Due to the presence of thermally responsive NIPAM units and varying molar ratios of anionic (AMPS) and cationic (APTAC) units, the resulting nanogels were responsive to multiple stimuli in aqueous media and can be used for controlled delivery of dyes. Thus, the $NIPAM_{90}$-$APTAC_{7.5}$-$AMPS_{2.5}$ nanogel with an excess of the cationic units was chosen for immobilization of the anionic dye, methyl orange (MO), whereas the $NIPAM_{90}$-$APTAC_{2.5}$-$AMPS_{7.5}$ nanogel with an excess of the anionic units was chosen for immobilization of the cationic dye, methylene blue (MB). The release kinetics of the dyes from the nanogel was studied depending on the phase transition temperature and the salt content. Mechanism of the dye release from the nanogel matrix was determined using the Ritger-Peppas equation. Disappearance of the ionic contacts between the charged groups of the nanogels and the ionic dyes was suggested to be the main reason for the diffusion of the dyes through the dialysis membrane into external solution.

Keywords: polyampholyte nanogels, methyl orange, methylene blue, polyampholyte-dye complex, phase transition temperature, dye release.

Introduction

Interaction between polyelectrolytes and low molar mass ionic dyes leads to the formation of polyelectrolyte-dye complexes with modified physical and chemical properties. The main driving force for this complexation is electrostatic binding. To develop novel materials with desired properties, which can be used in chemical separation, drug delivery or waste treatment, it is necessary to deepen understanding of the molecular interactions between dyes and polyelectrolytes.

Thus, the effect of the molecular architecture of synthetic polycations has been demonstrated using a complex formed between anionic dye, methyl orange (MO), and either linear strongly charged poly(diallyl dimethyl amine hydrochloride) (PDADMAC) or branched poly(ethyleneimine hydrochloride) (PEI). The complex formation is first determined by long-range electrostatic interactions accompanied with hydrophobic and π-π interactions on shorter distances [1].

Bernards *et al*. [2] has described the release of three pseudodrug molecules (caffeine, methylene blue or methanil yellow) from an nonfouling polyampholyte hydrogel based on [2-(acryloyloxy)ethyl]trimethyl-ammonium chloride (TMA) and 2-carboxyethyl acrylate (CAA) depending on the density of the hydrogel, crosslinking agent, pH and the ionic strength (μ) of the solution. Release of the neutral caffeine molecule is influenced only by diffusion, while the release of the charged methylene blue (MB) or methanil yellow is controlled by their interaction with the charged groups of TMA and CAA. pH and μ clearly influence the rate and degree of release of the charged pseudodrugs.

Cryogels based on sulfobetaine monomer 2-(N-3-sulfopropyl-N,N-dimethyl ammonium)ethyl methacrylate and dicationic crosslinking agent N,N,N',N'-tetramethyl-N,N'-bis(2-ethylmethacrylate)-propyl-1,3-diammonium dibromide are effective adsorbents for MO and MB [3]. The degree of MO adsorption is higher

than that of MB, and hence, anionic dyes may have a higher probability of being captured by the cryogel. Sulfobetaine groups have an advantage based on the stabilization of the hydrogel structure, which can be used in wastewater treatment [4].

Polyelectrolyte membranes, which remain solvated and functional in concentrated salt solutions or under strong acidic/basic conditions, are widely applied to separate dyes from wastewater by adjusting the polyelectrolyte-dye interaction [5–7]. For example, interactions between poly(2-acrylamide-2-methyl-1-propanesulfonic acid) (PAMPS) and poly(diallyldimethylammonium) chloride (PDDA) and cationic dyes MB and MO have been used to treat colored wastewater by polymer-enhanced ultrafiltration method (PEUF) [8].

Polyampholyte microgels based on the N-isopropylacrylamide backbone containing methacrylic acid and 2-(dimethylamino)ethyl methacrylate have been used to absorb and release cationic surfactants. Depending on the type of surfactant and pH of the medium, the absorption mechanism is determined by a combination of electrostatic and hydrophobic interactions as well as H-bonding [9].

Despite of some progress in the field of complex formation between polyelectrolytes and dyes, there is little information about complexes formed between amphoteric nanogels and dyes. In our previous study, the interaction of polyampholyte hydrogels consisting of (3-acrylamidopropyl) trimethylammonium chloride (APTAC) and sodium salt of 2-acrylamido-2-methyl-1-propanesulfonic acid (AMPS) with MB and MO was investigated. Hydrogels containing an excess of negative and positive charges effectively absorb up to 80–90 % of dyes owing to the electrostatic binding [10]. In this article, we describe synthesis and characterization of polyampholyte nanogels based on neutral N-isopropylacrylamide (NIPAM), anionic sodium salt of 2-acrylamido-2-methyl-1-propanesulfonic acid (AMPS) and cationic (3-acrylamidopropyl)trimethyl-ammonium chloride (APTAC). Resulting nanogels have random distribution of repeating units, where 90 mol. % of NIPAM units bring in thermoresponsive behavior to the nanogels, while AMPS and APTAC provide electrostatic interaction. We investigate the immobilization of anionic and cationic dyes within the matrix of amphoteric nanogels and study the release kinetics of these dyes from the nanogel matrix as a function of temperature and salt concentration.

Experimental

Materials

Monomers — N-isopropylacrylamide (NIPAM, 97 % purity), 2-acrylamido-2-methylpropanesulfonic acid sodium salt (AMPS, 50 wt. %) and (3-acrylamidopropyl) trimethylammonium chloride (APTAC, 75 wt. %); the redox initiator — ammonium persulfate (APS, 98 % purity) and sodium metabisulfite (SMBS, 97 % purity); the surfactant — sodium dodecyl sulfate (SDS, 99 % purity); the crosslinker — N,N-methylenebis(acrylamide) (MBAA, 99 % purity); sodium chloride (NaCl); dialysis tubing cellulose membrane (12–14 kDa); anionic dye — methyl orange (MO, $\lambda_{max} = 464$ nm); cationic dye — methylene blue (MB, $\lambda_{max} = 662$ nm) were purchased from Sigma-Aldrich Chemical Co. and used as received.

Synthesis of nanogels based on NIPAM-APTAC-AMPS

Polyampholyte nanogels of various compositions $NIPAM_{90}-APTAC_{7.5}-AMPS_{2.5}$ and $NIPAM_{90}-APTAC_{2.5}-AMPS_{7.5}$ were synthesized via conventional redox initiated free radical copolymerization (Scheme 1).
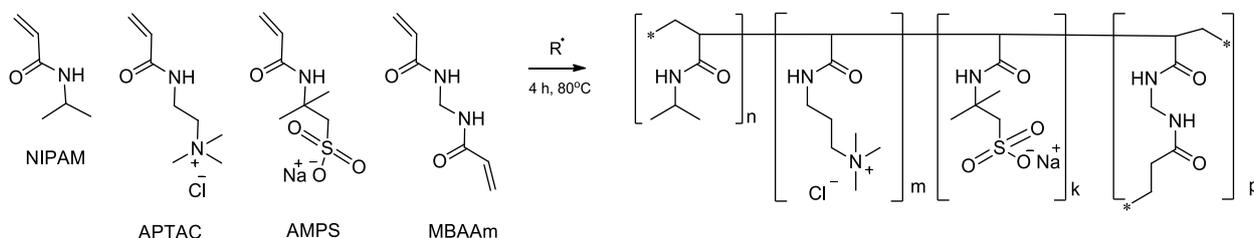
Scheme 1. Free radical copolymerization of NIPAM, APTAC and AMPS monomers for synthesis of nanogels $NIPAM_{90}-APTAC_{7.5}-AMPS_{2.5}$ and $NIPAM_{90}-APTAC_{2.5}-AMPS_{7.5}$

To obtain the nanogels, required amounts of monomers NIPAM, APTAC and AMPS, MBAA as crosslinker, and SDS as surfactant were dissolved in deionized water with constant stirring until complete dissolu-

tion of the components (Table 1). Required amounts of APS and SMBS were added to this solution and stirred for 5 minutes. The solution was then transferred to a sealed round bottom flask. The conventional redox initiated free radical copolymerization was carried out at 80 °C for 4 h under argon atmosphere with constant stirring of the mixture. The obtained nanogel solutions were dialyzed in deionized water for 14 days to remove unreacted components.

Table 1

Polymerization protocol of NIPAM-APTAC-AMPS nanogels

Nanogel sample	NIPAM, g	APTAC, g	AMPS, g	APS, mg	MBAA, g	SMBS, mg	SDS, g	H_2O, mL	Yield, wt. %
$NIPAM_{90}$-$APTAC_{7.5}$-$AMPS_{2.5}$	0.735	0.149	0.082	20	0.11	10	0.35	98.5	88
$NIPAM_{90}$-$APTAC_{2.5}$-$AMPS_{7.5}$	0.735	0.049	0.248	30	0.11		0.23		72

Methods

Chemical structure of NIPAM-APTAC-AMPS nanogels were characterized using FTIR spectroscopy (Cary 660 FTIR, Agilent, USA). Measurements were carried out on freeze-dried nanogels at room temperature within the 500-4000 cm^{-1} range of wavenumbers. ^1H NMR spectra were collected with a JNN-ECA Jeol 400 spectrometer (frequency 400 MHz) using D_2O as a solvent. Dynamic light scattering (DLS) and zeta-potential measurements were implemented by means of Zetasizer Nano ZS 90 (Malvern, UK) with a 633 nm laser. Analysis of the surface morphology using MIRA 3 LMU scanning electron microscopy (Tescan, Czech Republic) was performed for 0.1 wt. % solution of nanogels after drying at 25 °C. Absorption spectra of MO and MB were registered with a UV-Vis spectrophotometer Specord 210 plus (Germany) at 25 °C.

Immobilization of dyes within the matrix of charge-imbalanced amphoteric nanogels

Immobilization of anionic dye, methyl orange (MO), and a cationic dye, methylene blue (MB), into the matrix of nanogels was performed as follows. 2.5 mL of 1 mM MO solution and 2.5 mL of 0.4 wt. % $NIPAM_{90}$-$APTAC_{7.5}$-$AMPS_{2.5}$ nanogel were poured to a 50 mL flask. Distilled water was then added up to the required volume. The final concentration of MO and $NIPAM_{90}$-$APTAC_{7.5}$-$AMPS_{2.5}$ nanogel in the flask was $5 \cdot 10^{-2}$ mM and 0.1 wt. %, respectively.

The MB immobilization is identical to the procedure described above: 2.5 mL of 1 mM MB and 2.5 mL of 0.4 wt. % $NIPAM_{90}$-$APTAC_{2.5}$-$AMPS_{7.5}$ nanogel were poured into a 50 mL flask; the required amount of water was added obtaining $5 \cdot 10^{-2}$ mM MB and 0.1 wt.% $NIPAM_{90}$-$APTAC_{2.5}$-$AMPS_{7.5}$ nanogel.

The $NIPAM_{90}$-$APTAC_{7.5}$-$AMPS_{2.5}$ nanogel with an excess of the positively charged APTAC monomer was chosen for the immobilization of the MO anionic dye. Whereas the $NIPAM_{90}$-$APTAC_{2.5}$-$AMPS_{7.5}$ nanogel with an excess of the negatively charged AMPS monomer was chosen for immobilization of the cationic dye MB. Since the determination of the composition of the nanogel-dye complexes presents a certain experimental difficulty, we first carried out the conductometric titration of an aqueous solution of the linear terpolymer $NIPAM_{90}$-$APTAC_{7.5}$-$AMPS_{2.5}$ with the anionic dye MO and the linear terpolymer $NIPAM_{90}$-$APTAC_{2.5}$-$AMPS_{7.5}$ with the cationic dye MB at polymer concentrations $1 \cdot 10^{-1}$ mM and dye concentrations 1 mM (Figure 1).

In case of the $NIPAM_{90}$-$APTAC_{7.5}$-$AMPS_{2.5}$ linear terpolymer, the inflection point corresponds to the composition of the complex [$NIPAM_{90}$-$APTAC_{7.5}$-$AMPS_{2.5}$]/[MO] = 1:0.8 mol/mol, which is close to the equimolar ≈ 1:1. In case of the $NIPAM_{90}$-$APTAC_{2.5}$-$AMPS_{7.5}$ system, the inflection point corresponds to the composition of the complex [$NIPAM_{90}$-$APTAC_{2.5}$-$AMPS_{7.5}$]/[MB] = 1:1 mol/mol. Thus, linear NIPAM-APTAC-AMPS polyampholytes with an excess of positive (APTAC) or negative (AMPS) monomers form 1:1 equimolar complex with ionic dyes (MO and MB). For this reason, further study of the dyes release from the volume of the NIPAM-APTAC-AMPS nanogels was carried out for equimolar nanogel-dye compositions found for linear polyampholytes.

The electrostatic binding of anionic and cationic dyes by charged groups of amphoteric nanogels NIPAM-APTAC-AMPS with release of NaCl is represented in Figure 2.
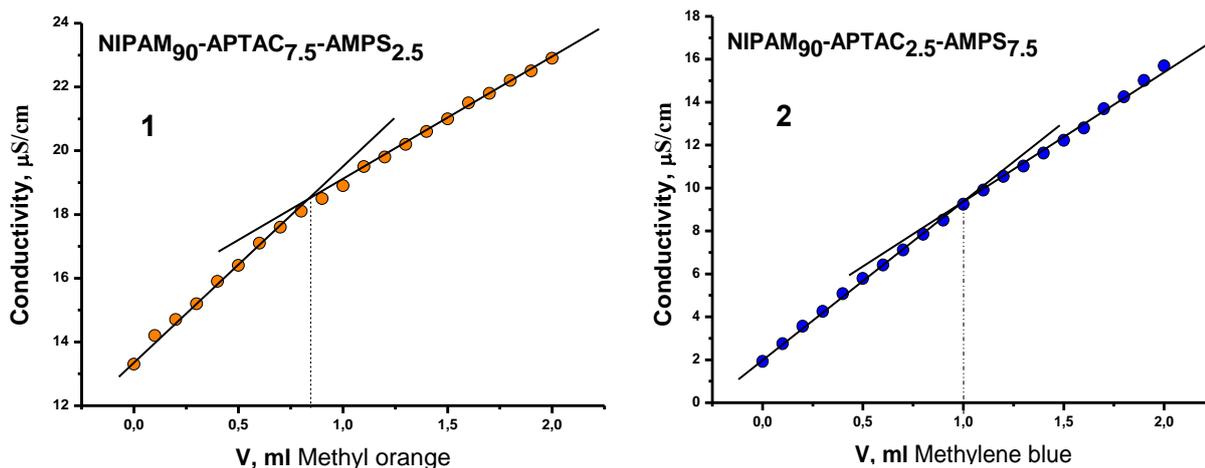
Figure 1. Conductometric titration of linear terpolymer NIPAM$_{90}$-APTAC$_{7.5}$-AMPS$_{2.5}$
with anionic dye MO (1) and linear terpolymer NIPAM$_{90}$-APTAC$_{2.5}$-AMPS$_{7.5}$ with cationic dye MB (2)
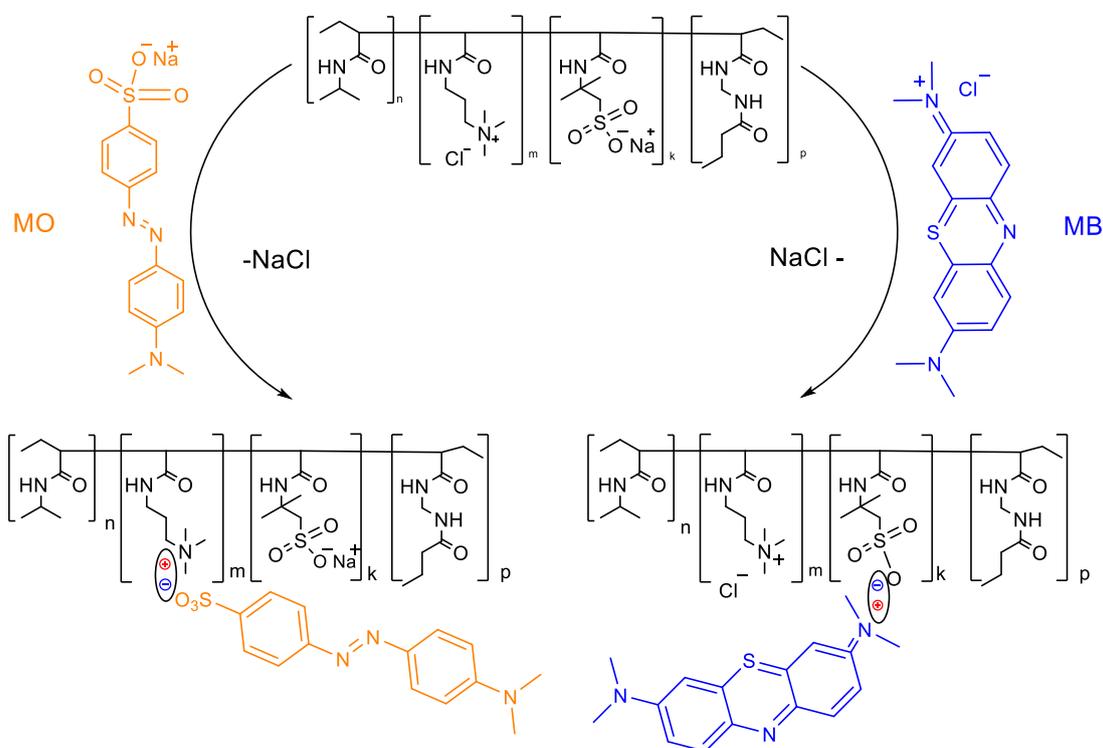at a polymer concentration of $1 \cdot 10^{-1}$ mM and concentration dyes 1 mM

Figure 2. Formation of equimolar complexes between amphoteric nanogels and ionic dyes

Determination of phase transition temperatures for NIPAM-APTAC-AMPS nanogels

The phase transition temperatures (T$_{p.t.t.}$) of nanogels based on NIPAM-APTAC-AMPS in aqueous and aqueous-salt solutions were determined by observing the change in transmittance of the solution upon increasing temperature. Below the lower critical solution temperature (LCST), aqueous and aqueous-salt solutions of NIPAM-APTAC-AMPS nanogels are transparent. The solutions become milky white above the LCST, when the polymer dehydrates and becomes more hydrophobic hence less soluble in water and transmittance decreases. Phase transition experiments were carried out at $\lambda = 700$ nm at a NIPAM-APTAC-AMPS nanogel concentration of 0.1 wt.%, heating rate 0.5°C min^{-1} and at the temperature range of 25–60°C, as described in [11]. T$_{p.t.t.}$ of NIPAM-APTAC-AMPS nanogels in aqueous NaCl solutions with the ionic strength $\mu = 1$; $1 \cdot 10^1$; $1 \cdot 10^2$; $5 \cdot 10^2$ and $1 \cdot 10^3$ mM correspond to the minimum points on differential curves.

Examples are shown in Figure 3 for the $NIPAM_{90}$-$APTAC_{7.5}$-$AMPS_{2.5}$ nanogel at different μ. Figure 3 demonstrates that added salt screens charges of the polymers. When $\mu = 1 \cdot 10^3$ mM, electrostatic interaction is totally screened and the nanogels behave similar to pure PNIPAM. For the $NIPAM_{90}$-$APTAC_{2.5}$-$AMPS_{7.5}$ nanogel, the experiments were carried out identically.
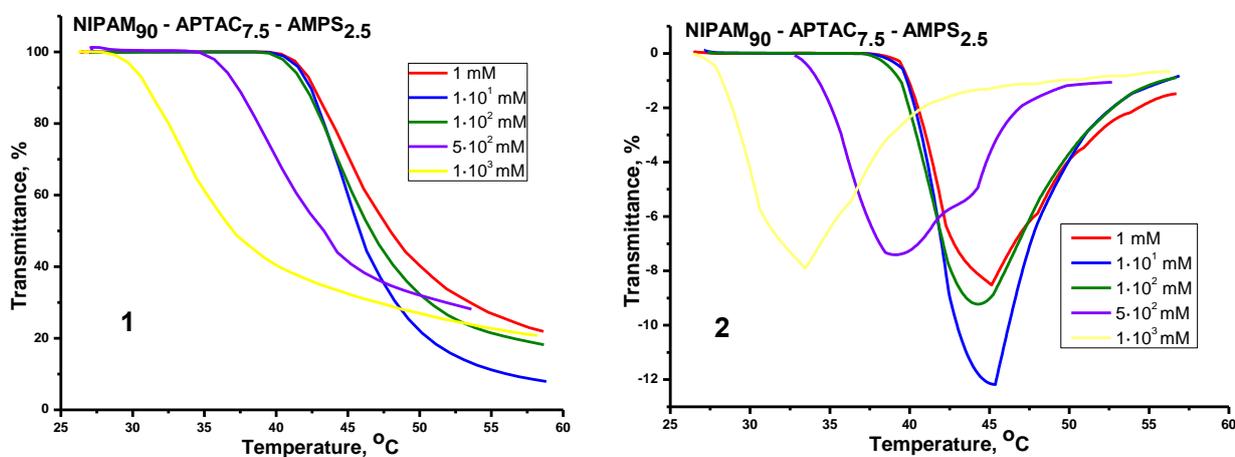
Figure 3. Integral (*1*) and differential (*2*) curves of temperature-dependent phase behavior of the nanogel $NIPAM_{90}$-$APTAC_{7.5}$-$AMPS_{2.5}$ at different μ

Release of dyes from NIPAM-APTAC-AMPS nanogels

The release (or diffusion to the outer solution) of dyes was carried out using a simple "glass in a glass" device with constant stirring, shown in Figure 4. For this, the inner glass, the bottom of which was covered with a dialysis membrane (molecular weight cut off is 12-14 kDa), was filled with a mixture of 10 mL of dye (MO or MB) with $5 \cdot 10^{-2}$ mM concentration and 0.1 wt. % of nanogel ($NIPAM_{90}$-$APTAC_{2.5}$-$AMPS_{7.5}$ or $NIPAM_{90}$-$APTAC_{7.5}$-$AMPS_{2.5}$). It was dipped to the outer vessel containing 20 mL of distilled water or aqueous NaCl solution ($\mu = 1, 1 \cdot 10^1$ and $1 \cdot 10^2$ mM). All measurements were carried out under stirring at 25 °C and at $T_{p.t.t.}$ of nanogels determined as described above. Covering the bottom part of the inner glass with a dialysis membrane retains the nanogel in the inner vessel and keeps the concentration of nanogel constant. At the same time, pores of the dialysis membrane did not prevent diffusion of the released dye molecules (MB or MO) into the outer beaker. At certain time intervals, 2 mL of sample was taken from the outer beaker for the UV-Vis analysis. The experiments were performed under the sink conditions: to keep the volume of the solution constant, the 2 mL solution taken for analysis was compensated by adding 2 mL of distilled water or aqueous-salt solution.
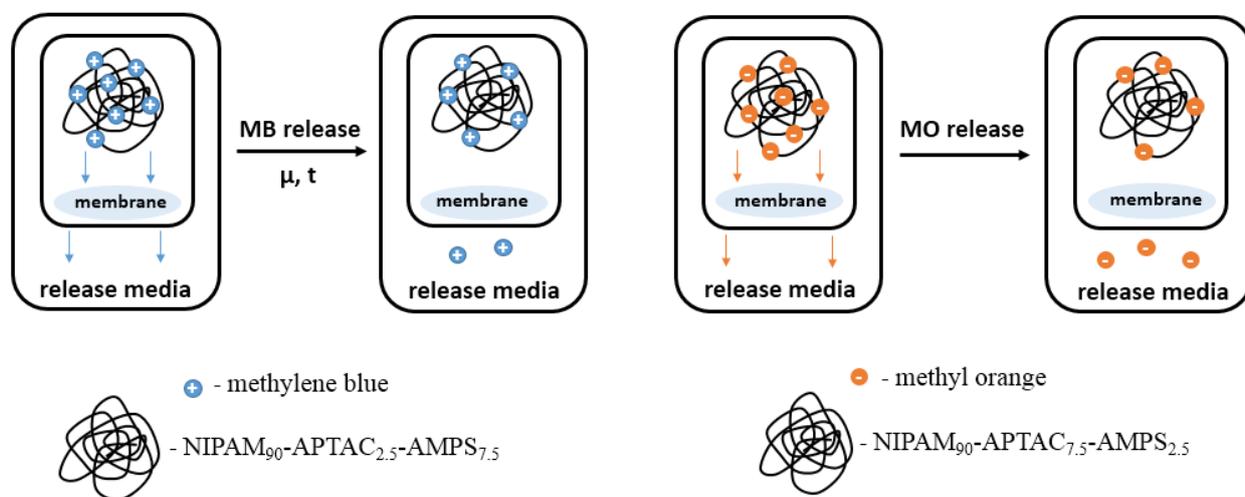
Figure 4. "Glass-in-glass" device for dye release from the nanogel matrix

The concentration of the dyes released into distilled water or aqueous-salt solutions was determined using a UV-Vis spectrophotometer at 464 nm for MO and 662 nm for MB and expressed by Equation 1:

$$\text{Dye release (\%)} = \frac{[\text{released dye}]}{[\text{total dye}]} \cdot 100. \tag{1}$$

Dye release kinetics

Kinetics and mechanism of the dye release from the nanogel matrix was determined using the Ritger-Peppas model for simple solute release, which is described by Equation 2 [12]:

$$M_t / M_\infty = kt^n, \tag{2}$$

where M_t — is the concentration of dye released at time t; M_∞ — is the concentration of dye at infinite time t_∞; k — is the kinetic constant; n — is the exponent of diffusion indicating the mechanism of dye transport from the nanogel matrix.

The values of n can be the following: when $n = 0.5$, diffusion is the main driving force (Fickian diffusion); when $n = 1$, the dye release is largely controlled by degradation (Case II transport); when $0.5 < n < 1.0$, the dye release is followed by both diffusion and erosion controlled mechanisms (non-Fickian diffusion or anomalous mechanism of the drug release).

The cumulative release was calculated by Equation 3 [13]:

$$\text{Cumulative percentage release, \%} = \frac{\text{Volume of sample withdrawn, mL}}{\text{Bath volume, mL}} \; P_{(t-1)} + P_t, \tag{3}$$

where P_t — is percentage release at time t; $P_{(t-1)}$ — is percentage release previous to t.

Results and Discussion

Synthesis and characterization of nanogels based on NIPAM-APTAC-AMPS

$NIPAM_{90}$-$APTAC_{7.5}$-$AMPS_{2.5}$ and $NIPAM_{90}$-$APTAC_{2.5}$-$AMPS_{7.5}$ nanogels were synthesized via conventional redox initiated free radical copolymerization. Two molar ratios of the anionic (AMPS) and cationic (APTAC) monomers were used to obtain the suitable stimuli-responsive systems with optimal properties for controlled dye release studies.

FTIR analysis of the nanogels

Figure 5 represents the FTIR spectra of NIPAM-APTAC-AMPS nanogels. The characteristic peaks of the functional groups found at $\nu = 3290$–3500 cm^{-1} belong to the secondary and tertiary amine groups. Peaks at $\nu = 2800$–3000 cm^{-1} and 1460 cm^{-1} are responsible for the CH groups. Peaks at $\nu = 1640$ and 1540 cm^{-1} are attributed to the N-substituted groups (amide I and amide II). S=O groups containing in AMPS fragments appear at $\nu = 1040$ cm^{-1}.
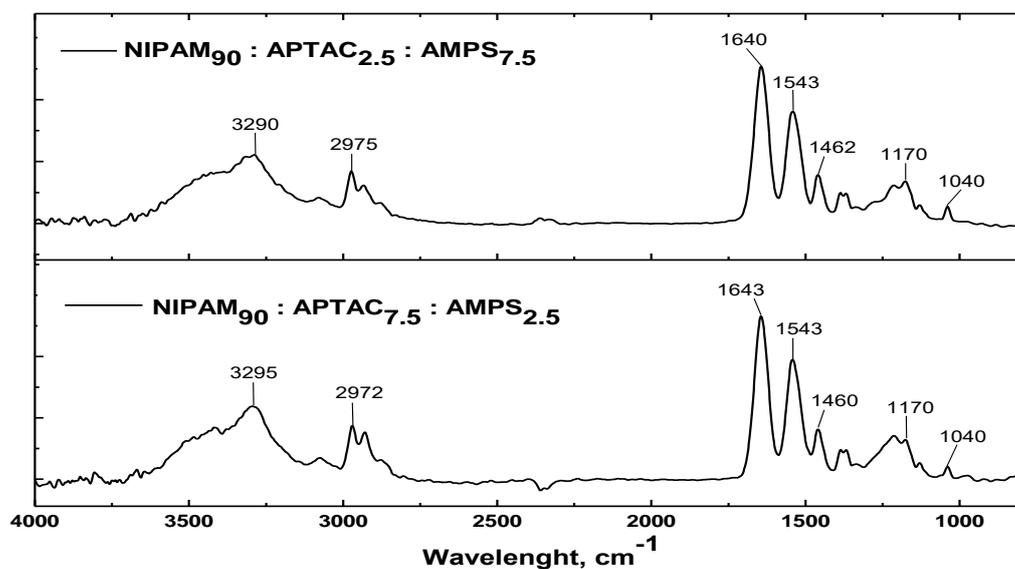

Figure 5. FTIR spectra of NIPAM-APTAC-AMPS nanogels

¹H NMR analysis of nanogels

The methylene and methine protons include resonance bands at 1.8 and 2.2 ppm, which also overlap with the peaks of the methyl and methylene protons of AMPS and APTAC. The suspended protons of the methyl and methylene groups in AMPS and APTAC include resonance bands at 3.2–3.4 ppm. Since these signals overlapped, the exact composition of the $NIPAM_{90}$-$APTAC_{7.5}$-$AMPS_{2.5}$ and $NIPAM_{90}$-$APTAC_{2.5}$-$AMPS_{7.5}$ nanogels could not be accurately determined from the ¹H NMR spectra (Figure 6). One should note that reactivities of used monomers is the same and close to one. Therefore, it can be assumed that the ratio of the reacted repeating units in the nanogels is practically the same as that of the monomers in feed [14]. Taking into account all the reasons above, it can be argued that the $NIPAM_{90}$-$APTAC_{7.5}$-$AMPS_{2.5}$ and $NIPAM_{90}$-$APTAC_{2.5}$-$AMPS_{7.5}$ nanogels containing an excess of positively (APTAC) or negatively (AMPS) charged monomers are charge imbalanced.
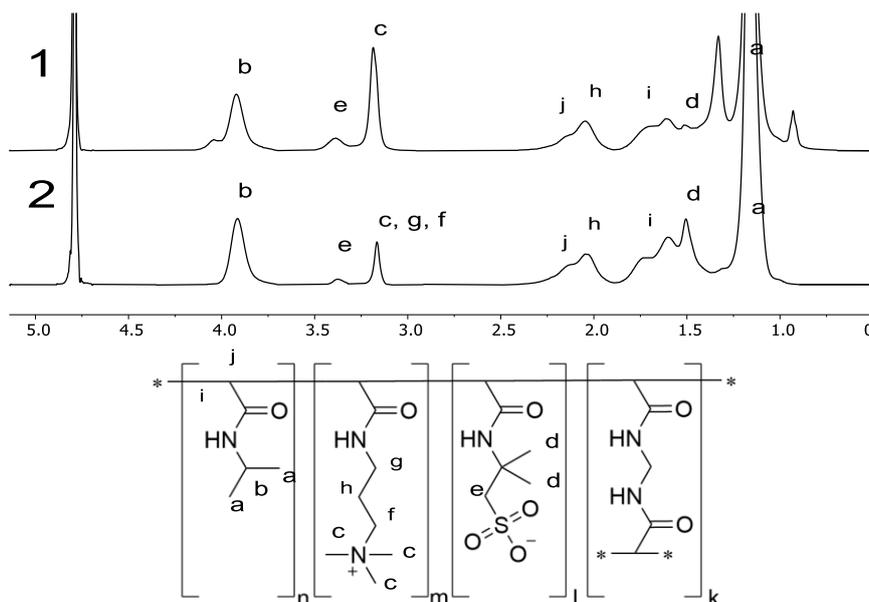

Figure 6. NMR spectra of $NIPAM_{90}$-$APTAC_{7.5}$-$AMPS_{2.5}$ (1) and $NIPAM_{90}$-$APTAC_{2.5}$-$AMPS_{7.5}$ (2) nanogels and identification of proton signals

The mean hydrodynamic radius (R_h) and zeta-potentials (ζ) of NIPAM-APTAC-AMPS nanogels in aqueous and aqueous-salt solutions

The mean hydrodynamic size was measured in a 0.1 wt.% solution of nanogels in the temperature range from 25 to 50 °C with an interval of 5 °C in DI water and in NaCl solutions with $\mu = 1$, $1 \cdot 10^1$ and $1 \cdot 10^2$ mM (Table 2).

T a b l e 2

The mean hydrodynamic size of NIPAM-APTAC-AMPS nanogels

T, °C	Hydrodynamic radius (R_h), nm							
	$NIPAM_{90}$-$APTAC_{7.5}$-$AMPS_{2.5}$				$NIPAM_{90}$-$APTAC_{2.5}$-$AMPS_{7.5}$			
	μ, mol·L⁻¹ (NaCl)							
	0	1	$1 \cdot 10^1$	$1 \cdot 10^2$	0	1	$1 \cdot 10^1$	$1 \cdot 10^2$
25	6.5±1	8±2	8±1	90 ±12	14±1 275±20*	14±2 480±8*	11±1	11±1 160±20*
30	9±1	9±2	7 ±0.5	138±10	13±1 330±20*	12±2 735±10*	13±0.5	120±10
35	8±3	7±1	7±1	197±1	565±15	740±10	265±20	170±1
40	68±4	90±8	115±9	220±10	570±10	744±4	270±20	172±1
45	110±0.5	148±0.5	196±1.5	201±5	110±1.5	265±1	650±15	172±2
50	127±0.5	171±0.5	201±7	200±3	135±5	307±0.5	690±10	410±20
* nanogels in some solutions have a bimodal distribution.								

Zeta-potentials of charge-imbalanced NIPAM-APTAC-AMPS nanogels were measured in 0.1 wt.% aqueous solution at 25 °C. An aqueous solution of $NIPAM_{90}$-$APTAC_{7.5}$-$AMPS_{2.5}$ with an excess of positively charged APTAC monomer has $\zeta = +4\pm1$ mV. $NIPAM_{90}$-$APTAC_{2.5}$-$AMPS_{7.5}$ with an excess of negatively charged AMPS monomer has $\zeta = -7\pm1$ mV.

SEM analysis of the nanogels

As is seen from SEM image, the nanogel particles contain glued or stuck aggregates (Figure 7). The narrow necks connecting the nanogel particles and few nanometer- and micron-sized voids are clearly visible. Macroscopic gelation occurs due to multiple contacts between spherical or wormlike nanogels, which lead to the formation of a three-dimensional network of nanogels [15].
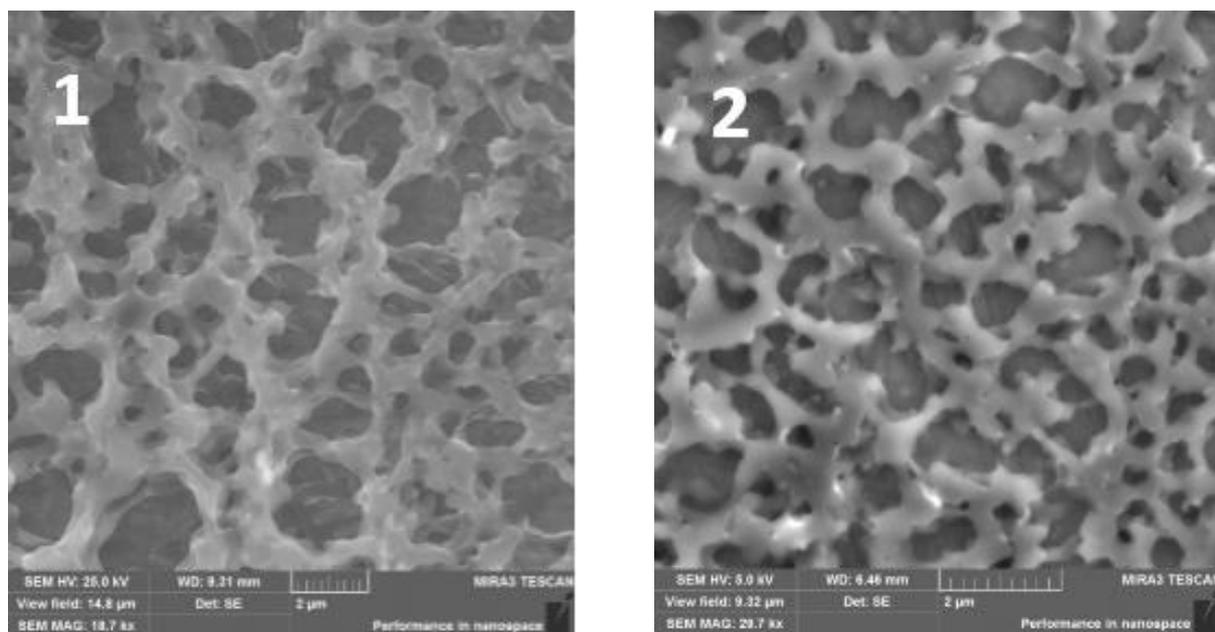

Figure 7. SEM images of $NIPAM_{90}$-$APTAC_{7.5}$-$AMPS_{2.5}$ (*1*) and $NIPAM_{90}$-$APTAC_{2.5}$-$AMPS_{7.5}$ (*2*) nanogels

Release kinetics of dyes from the matrix of charge-imbalanced amphoteric nanogels

Figure 8 shows the cumulative of release of MO from nanogel $NIPAM_{90}$-$APTAC_{7.5}$-$AMPS_{2.5}$ into deionized water and aqueous-salt solution containing 1, $1\cdot10^1$ and $1\cdot10^2$ mM NaCl. The released amount of MO from the nanogel matrix is summarized in Table 3.
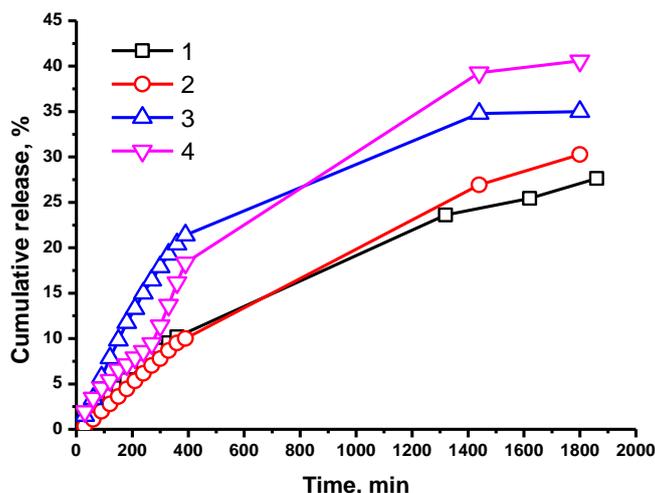
1 — DI water; *2* — 1 mM NaCl; *3* — $1\cdot10^1$ mM NaCl; *4* — $1\cdot10^2$ mM NaCl. [MO] = $5\cdot10^{-2}$ mM

Figure 8. Cumulative release of MO from $NIPAM_{90}$-$APTAC_{7.5}$-$AMPS_{2.5}$ nanogel at 25 °C in different media

The equilibrium release data of MO for nanogel NIPAM₉₀-APTAC₇.₅-AMPS₂.₅ at 25°C

μ, mol·L⁻¹ (NaCl)	Released amount of MO during 30 h, (%)
0	27.0±0.5
1	30.0±0.5
$1 \cdot 10^1$	35.0±0.5
$1 \cdot 10^2$	41.0±0.5

Gradually increasing MO release into the external solution is associated with destruction of the electrostatic interactions between the anionic groups of nanogel and the cationic dye upon increasing μ.

The release kinetics of MO from nanogel NIPAM₉₀-APTAC₇.₅-AMPS₂.₅ were fit using the Ritger–Peppas equation. The values of n and k are presented in Table 4. The values of n in DI water, 1 and $1 \cdot 10^1$ mM NaCl are around 1 and indicating case II transport release mechanism. When MO is released into $1 \cdot 10^2$ mM NaCl the n value equals 0.69, which indicates non-Fickian (anomalous) diffusion.

The values of n and k of MO for nanogel NIPAM₉₀-APTAC₇.₅-AMPS₂.₅ at 25 °C

Release medium	n	k·10²	Release mechanism
MO+NIPAM₉₀-APTAC₇.₅-AMPS₂.₅ into DI water	1.04±0.02	0.09	Case II transport
MO+NIPAM₉₀-APTAC₇.₅-AMPS₂.₅ into 1 mM NaCl	1.12±0.02	0.05	Case II transport
MO+NIPAM₉₀-APTAC₇.₅-AMPS₂.₅ into $1 \cdot 10^1$ mM NaCl	1.03±0.02	0.16	Case II transport
MO+NIPAM₉₀-APTAC₇.₅-AMPS₂.₅ into $1 \cdot 10^2$ mM NaCl	0.69±0.02	0.50	non-Fickian diffusion

The release kinetics of MB from NIPAM₉₀-APTAC₂.₅-AMPS₇.₅ nanogel was studied in aqueous-salt solutions at $\mu = 1$, $1 \cdot 10^1$ and $1 \cdot 10^2$ mM NaCl (Figure 9). When $\mu = 1$ and $1 \cdot 10^1$ mM NaCl (up to 400 min), the intensive diffusion of MB from the nanogel matrix is observed. This owes to the step-by-step destruction of the nanogel-dye complex due to screening of the negative charges of the nanogel by NaCl ions. At time interval from 400 to 1600 min, the MB diffusion rate reaches a plateau. This indicates the stationary nature of the release of the dye molecules from the bulk of the nanogel. At $\mu = 1 \cdot 10^2$ mM NaCl the rate of the dye diffusion from the nanogel matrix increases linearly, but after 1400 and 1600 min it reaches the limit value.
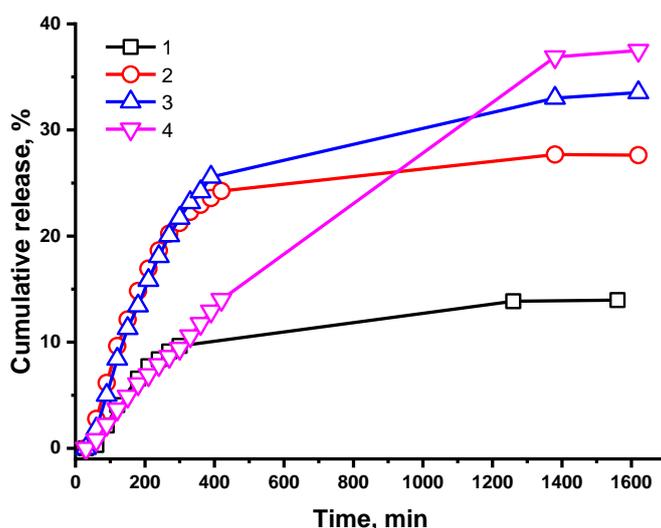
1 — DI water; *2* — 1 mM NaCl; *3* — $1 \cdot 10^1$ mM NaCl; *4* — $1 \cdot 10^2$ mM NaCl

Figure 9. Cumulative release of MB from NIPAM₉₀-APTAC₂.₅-AMPS₇.₅ nanogel in different media at 25 °C

The released amount of MB from the nanogel matrix is summarized in Table 5.

The equilibrium release data of MB for nanogel NIPAM$_{90}$-APTAC$_{2.5}$-AMPS$_{7.5}$ at 25 °C

| μ, mol·L^{-1} (NaCl)	Released amount of MB during 27 h, (%)
0	14.0±0.5
1	28.0±0.5
1·10^1	34.0±0.5
1·10^2	37.0±0.5

The values of *n* equal one upon release of MB from the NIPAM$_{90}$-APTAC$_{2.5}$-AMPS$_{7.5}$ nanogel into deionized water and 1·10^2 mM NaCl solution indicating that the release mechanism is controlled by degradation, whereas the release into 1 and 1·10^1 mM NaCl corresponds to the diffusion and erosion-controlled mechanism (Table 6).

The values of *n* and *k* for release of MB for nanogel NIPAM$_{90}$-APTAC$_{2.5}$-AMPS$_{7.5}$ at 25 °C

Release medium	n	k·10^2	Release mechanism
MB+NIPAM$_{90}$-APTAC$_{2.5}$-AMPS$_{7.5}$ into DI water	1.2±0.02	0.76	Case II transport
MB+NIPAM$_{90}$-APTAC$_{2.5}$-AMPS$_{7.5}$ into 1 mM NaCl	0.7±0.02	1.25	non-Fickian diffusion
MB+NIPAM$_{90}$-APTAC$_{2.5}$-AMPS$_{7.5}$ into 1·10^1 mM NaCl	0.9±0.02	0.32	non-Fickian diffusion
MB+NIPAM$_{90}$-APTAC$_{2.5}$-AMPS$_{7.5}$ into 1·10^2 mM NaCl	1.3±0.02	0.016	Case II transport

Figure 10 shows the cumulative release of MO from the NIPAM$_{90}$-APTAC$_{7.5}$-AMPS$_{2.5}$ nanogel into NaCl solutions at the phase transition temperatures measured during 5 hours.
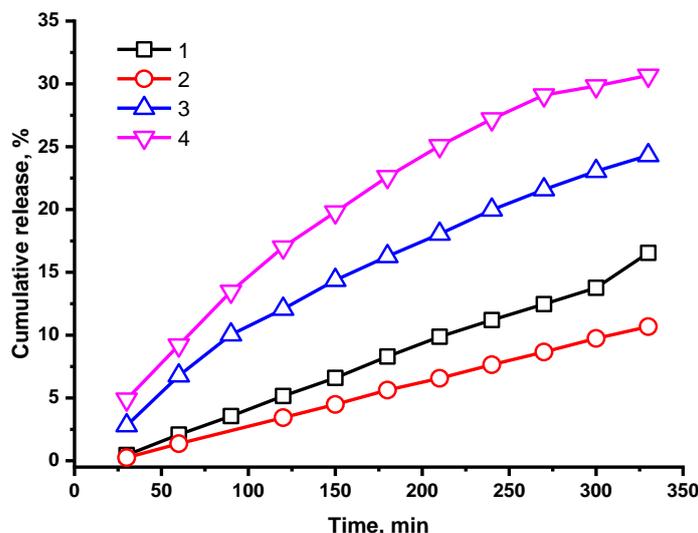
1 — DI water; *2* — 1 mM NaCl; *3* — 1·10^1 mM NaCl; *4* — 1·10^2 mM NaCl

Figure 10. Cumulative release of MO from NIPAM$_{90}$-APTAC$_{7.5}$-AMPS$_{2.5}$ nanogel in different media at T$_{p.t.t.}$

The effect of μ on the phase transition temperatures T$_{p.t.t.}$ and released amount of MO from NIPAM$_{90}$-APTAC$_{7.5}$-AMPS$_{2.5}$ nanogel is summarized in Table 7.

**Influence of the ionic strength (μ) on the phase transition temperatures ($T_{p.t.t.}$)
and released amount of MO from NIPAM$_{90}$-APTAC$_{7.5}$-AMPS$_{2.5}$ nanogel**

μ, mol·L^{-1} (NaCl)	Phase transition temperature, $T_{p.t.t.}$ (°C)	Released amount of MO during 5 h, (%)
0	44.0±0.1	17.0±0.5
1	45.1±0.1	11.0±0.5
$1·10^1$	44.4±0.1	24.0±0.5
$1·10^2$	44.3±0.1	31.0±0.5

The amount of released MO into deionized water at 44 °C equals 17 %. However, in a 1 mM solution at $T_{p.t.t.}$ = 45.1 °C it decreases down to 11 %. The released amount of MO into $1·10^1$ mM and $1·10^2$ mM solutions at $T_{p.t.t.}$ equals 24 and 31 % respectively. Therefore, an increase in temperature increases the MO release from the nanogel into deionized water, $1·10^1$ and $1·10^2$ mM NaCl solutions (Table 6).

The release of MO from nanogel matrix into $1·10^1$ mM salt solution at the phase transition temperature leads to a decrease in *n* down to 0.85 and the diffusion mechanism changes to non-Fickian (Table 8).

The values of *n* and *k* for release of MO for nanogel NIPAM$_{90}$-APTAC$_{7.5}$-AMPS$_{2.5}$ at $T_{p.t.t.}$

Release medium	n	$k·10^2$	Release mechanism
MO+NIPAM$_{90}$-APTAC$_{7.5}$-AMPS$_{2.5}$ into DI water	1.4±0.02	0.04	Case II transport
MO+NIPAM$_{90}$-APTAC$_{7.5}$-AMPS$_{2.5}$ into 1 mM NaCl	1.1±0.02	0.09	Case II transport
MO+NIPAM$_{90}$-APTAC$_{7.5}$-AMPS$_{2.5}$ into $1·10^1$ mM NaCl	0.85±0.02	0.08	non-Fickian diffusion
MO+NIPAM$_{90}$-APTAC$_{7.5}$-AMPS$_{2.5}$ into $1·10^2$ mM NaCl	0.77±0.02	1.3	non-Fickian diffusion

The effect of the phase transition temperature on the MB release from the NIPAM$_{90}$-APTAC$_{2.5}$-AMPS$_{7.5}$ nanogel is shown in Figure 11. The dye release in deionized water did not change during 5 hours as the temperature increased from 25 to 41.6 °C. The diffusion of MB from the nanogel into NaCl solutions with different μ = 1, $1·10^1$ and $1·10^2$ mM at the phase transition temperature increases by 7–15 % (Table 9).
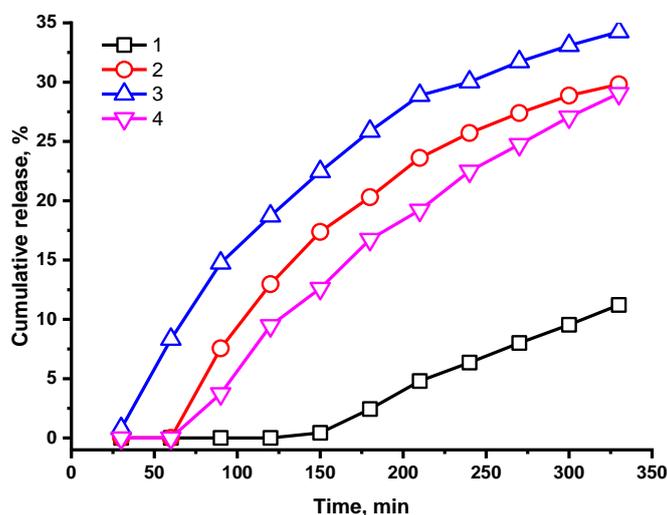
1 — DI water; *2* — 1 mM NaCl; *3* — $1·10^1$ mM NaCl; *4* — $1·10^2$ mM NaCl

Figure 11. Cumulative release of MB from NIPAM$_{90}$-APTAC$_{2.5}$-AMPS$_{7.5}$ nanogel in different media at $T_{p.t.t.}$

Ta b l e 9

The equilibrium release data of MB for nanogel NIPAM$_{90}$-APTAC$_{2.5}$-AMPS$_{7.5}$ at T$_{p.t.t.}$

μ, mol·L^{-1} (NaCl)	Phase transition temperature, T$_{p.t.t.}$ (°C)	Release amount of MB during 5 hrs, (%)
0	41.6±0.1	11±0.5
1	40.8±0.1	30±0.5
1·10^1	41.8±0.1	34±0.5
1·10^2	41.4±0.1	29±0.5

The influence of T$_{p.t.t.}$ on the change in the diffusion mechanism occurred when the MB was released into a 1 M NaCl. The *n* value changed to 1 and the mechanism became - Case II transport (Table 10).

Ta b l e 1 0

The values of *n* and *k* for release of MB for nanogel NIPAM$_{90}$-APTAC$_{2.5}$-AMPS$_{7.5}$ at T$_{p.t.t.}$

Release medium	n	k·10^2	Release mechanism
MB+NIPAM$_{90}$-APTAC$_{2.5}$-AMPS$_{7.5}$ into 1 mM NaCl	1±0.04	0.33	Case II transport
MB+ NIPAM$_{90}$-APTAC$_{2.5}$-AMPS$_{7.5}$ into 1·10^1 mM NaCl	0.76±0.02	1.3	non-Fickian diffusion
MB+NIPAM$_{90}$-APTAC$_{2.5}$-AMPS$_{7.5}$ into 1·10^2 mM NaCl	1.2±0.02	0.063	Case II transport

Conclusions

Samples of polyampholyte nanogels NIPAM$_{90}$-APTAC$_{7.5}$-AMPS$_{2.5}$ and NIPAM$_{90}$-APTAC$_{2.5}$-AMPS$_{7.5}$ were obtained via conventional redox initiated free radical copolymerization in presence of a cross-linking agent. The structure and composition of the nanogels were investigated by means of IR-Fourier and ^{1}H NMR spectroscopy.

The kinetics of release of dyes from the matrix of nanogels has been studied in aqueous solutions at various temperatures and ionic strengths. The MO release from the NIPAM$_{90}$-APTAC$_{7.5}$-AMPS$_{2.5}$ nanogel matrix at 25 °C for 30 hours increases from 27 to 41 % with increasing μ. At the phase transition temperature, the release of MO with μ is preserved, except for 1 mM NaCl, for which the release is 11 % and less than in distilled water. The release of MB from the NIPAM$_{90}$-APTAC$_{2.5}$-AMPS$_{7.5}$ nanogel within 27 hours rises from 14 to 37 % with μ. The upward trend in the MB release with μ persists at the phase transition temperature as well.

Gradual increase in the dyes release of from the nanogel matrix into the external solution is associated with the destruction/screening of electrostatic interactions of the nanogel-dye complex with μ. The release of the dye molecules is enhanced at the phase transition temperature of nanogels. Dye delivery systems developed in this study may be the promising platforms for therapeutic applications.

Acknowledgments

References

1   Vleugels, L.F.W. (2018). Self-organization of polyelectrolytes : as mediated by surfactants, dyes and ions. Dissertation. Technische Universiteit Eindhoven.

2   Barcellona, M.N., Johnson N., & Bernards, M.T. (2015). Characterizing Drug Release from Nonfouling Polyampholyte Hydrogels. *Langmuir*, *31*(49), 13402–13409. https://doi.org/10.1021/acs.langmuir.5b03597

3   Ihlenburg, R. B. J., Lehnen, A.-C., Koetz, J., & Taubert, A. (2021). Sulfobetaine Cryogels for Preferential Adsorption of Methyl Orange from Mixed Dye Solutions. *Polymers,* 13(2), 208. https://doi.org/10.3390/polym13020208

4   Ihlenburg, R.B.J., Mai, T., Thünemann, A. F., Baerenwald, R., Saalwächter, K., Koetz, J., & Taubert, A. (2021). Sulfobetaine Hydrogels with a Complex Multilength-Scale Hierarchical Structure. *The Journal of Physical Chemistry B, 125*(13), 3398–3408. https://doi.org/10.1021/acs.jpcb.0c10601

5   Deen, G. R., Wei, T. T., & Fatt, L. K. (2016). New stimuli-responsive polyampholyte: Effect of chemical structure and composition on solution properties and swelling mechanism. *Polymer, 104*, 91–103. https://doi.org/10.1016/j.polymer.2016.09.094

6   Rabiee, A., Ershad-Langroudi, A., & Jamshidi, H. (2014). Polyacrylamide-based polyampholytes and their applications. *Reviews in Chemical Engineering, 30*(5). https://doi.org/10.1515/revce-2014-0004

7   Mi, L., & Jiang, S. (2012). Synchronizing nonfouling and antimicrobial properties in a zwitterionic hydrogel. *Biomaterials, 33*(35), 8928–8933. https://doi.org/10.1016/j.biomaterials.2012.09.011

8   Oyarce, E., Butter, B., Santander, P., & Sánchez, J. (2021). Polyelectrolytes applied to remove methylene blue and methyl orange dyes from water via polymer-enhanced ultrafiltration. *Journal of Environmental Chemical Engineering, 106297.* https://doi.org/10.1016/j.jece.2021.106297

9   Bradley, M., Vincent, B., & Burnett, G. (2008). Uptake and release of surfactants from polyampholyte microgel particles. *Colloid and Polymer Science, 287*(3), 345–350. https://doi.org/10.1007/s00396-008-1978-8

10   Toleutay, G., Dauletbekova, M., Shakhvorostov, A., & Kudaibergenov, S. (2019). Quenched Polyampholyte Hydrogels Based on (3-Acrylamidopropyl)trimethyl Ammonium Chloride and Sodium Salt of 2-Acrylamido-2-methyl-1-Propanesulfonic Acid. *Macromolecular Symposia, 385*(1), 1800160. https://doi.org/10.1002/masy.201800160

11   Ayazbayeva, A.Ye., Shakhvorostov, A.V., Seilkhanov, T.M., Aseyev, V.O., & Kudaibergenov, S.E. (2021). Synthesis and characterization of novel thermo- and salt-sensitive amphoteric terpolymers based on acrylamide derivatives. *Bulletin of the University of Karaganda – Chemistry*, 104(4), 9–20. https://doi.org/10.31489/2021Ch4/9-20

12   Ritger, P. L., & Peppas, N. A. (1987). A simple equation for description of solute release II. Fickian and anomalous release from swellable devices. *Journal of Controlled Release, 5*(1), 37–42. https://doi.org/10.1016/0168-3659(87)90035-6

13   Chandrasekaran, A.R., Jia, C.Y., Theng, C.S., Muniandy, T., Muralidharan S., & Dhanaraj, S.A. (2011). In vitro studies and evaluation of metformin marketed tablets-Malaysia. *Journal of Applied Pharmaceutical Science, 1*(5), 214–217.

14   Braun, O., Selb, J., & Candau, F. (2001). Synthesis in microemulsion and characterization of stimuli-responsive polyelectrolytes and polyampholytes based on N-isopropylacrylamide. *Polymer, 42(21),* 8499–8510. https://doi.org/10.1016/S0032-3861(01)00445-1

15   Lovett, J.R., Derry, M.J., Yang, P., Hatton, F.L., Warren, N.J., Fowlera, P.W., & Armes, S.P. (2018). Can percolation theory explain the gelation behavior of diblock copolymer worms? *Chemical Science*, 9(35), 7138-7144. https://doi.org/10.1039/c8sc02406e

А.Е. Аязбаева, С.З. Наурызова, В.О. Асеев, А.В. Шахворостов

Заряд бойынша теңгерімсіз амфотерлік наногельдердің матрицасына метил қызғылт сары мен метилен көк бояуларын иммобилизациялау және олардың температура мен иондық күшке байланысты босап шығу кинетикасын зерттеу

Гидрофобты (N-изопропилакриламид, НИПАМ), теріс зарядталған (2-акриламидо-2-метилпропан-сульфонат натрий тұзы, АМПС) және оң зарядталған (3-акриламидопропилтриметиламмоний хлориді, АПТАХ) мономерлерден тұратын өзара байланысқан полиамфолитті наногельдер N,N-метилен-бис(акриламид) айқастырғыш агент ретінде қолданып бос радикалды полимерлену жолымен синтезделді. Алынған наногельдер ИК-Фурье және ^{1}H ЯМР спектроскопиясы әдістерімен сипатталды, беттік морфология сканерлеу электронды микроскопия арқылы талданды. Термосезімтал NIPAM және анионды (АМПС) және катионды (АПТАХ) мономерлердің әртүрлі молярлық коэффи-циенттерінің арқасында алынған наногельдер ынталандыруға сезімтал жүйелер болып табылады және оларды бояғыштарды бақыланатын түрде жеткізу үшін пайдалануға болады. Артық катионды мономері бар $NIPAM_{90}$-$APTAC_{7.5}$-$AMPS_{2.5}$ наногель анионды бояуды, метил қызғылт сарыны (MO), инкапсуляциялау үшін таңдалды, ал артық анионды мономері бар $NIPAM_{90}$-$APTAC_{2.5}$-$AMPS_{7.5}$ наногель катионды бояуды, метилен көк (MB), иммобилизациялау үшін таңдалды. Фазалық ауысу температурасына және тұз қоспасына байланысты наногельдің матрицасынан бояғыштардың шығарылу кинетикасы зерттелді, Ритгер-Пеппас теңдеуі негізінде наногель матрицасынан бояғыштың шығарылу механизмі анықталды. Зарядталған наногельдер топтары мен иондық бояғыштардың арасындағы иондық байланыстардың бұзылуы диализ мембранасы арқылы бояғыштардың сыртқы ерітіндіге таралуының негізгі себебі болып табылады.

Кілт сөздер: полиамфолит наногелі, метил қызғылт сары, метилен көк, полиамфолит-бояғыш кешені, фазалық ауысу температурасы, бояғышты босату.

А.Е. Аязбаева, С.З. Наурызова, В.О. Асеев, А.В. Шахворостов

Иммобилизация метилового оранжевого и метиленового синего в матрицу амфотерных наногелей с несбалансированным зарядом и изучение кинетики высвобождения красителей в зависимости от температуры и ионной силы

Сшитые полиамфолитные наногели, состоящие из гидрофобного (N-изопропилакриламид, НИПАМ), отрицательно заряженного (натриевая соль 2-акриламидо-2-метилпропансульфоната, АМПС) и положительно заряженного (3-акриламидопропилтриметиламмония хлорид, АПТАХ) мономеров, были синтезированы методом свободнорадикальной полимеризации с N,N-метиленбис(акриламидом) (МБАА) в качестве сшивающего агента. Полученные наногели охарактеризованы методами ИК-Фурье и ^{1}Н ЯМР спектроскопии, морфология поверхности проанализирована с помощью сканирующей электронной микроскопии. Из-за присутствия термочувствительного НИПАМ и различных молярных соотношений анионных (АМПС) и катионных (АПТАХ) мономеров, полученные наногели представляют собой стимул-чувствительные системы и могут использоваться для контролируемой доставки красителей. Наногель с избытком катионного мономера (NIPAM$_{90}$-APTAC$_{7.5}$-AMPS$_{2.5}$) был выбран для инкапсулирования анионного красителя метилового оранжевого (МО), а наногель с избытком анионного мономера (NIPAM$_{90}$-APTAC$_{2.5}$-AMPS$_{7.5}$) был выбран для иммобилизации катионного красителя метиленового синего (МС). Исследована кинетика высвобождения красителей из объема наногеля в зависимости от температуры фазового перехода и солевой добавки, определен механизм высвобождения красителей из матрицы наногеля на основе уравнения Ритгера-Пеппаса. Разрушение ионных контактов между заряженными группами наногелей и ионогенными красителями является основной причиной диффузии красителей через диализную мембрану во внешний раствор.

Ключевые слова: полиамфолитные наногели, метиловый оранжевый, метиленовый синий, комплекс полиамфолит-краситель, температура фазового перехода, высвобождение красителя

Information about authors[*]

Ayazbayeva, Aigerim Yerlanovna (*corresponding author*) — PhD student, Satbayev University, Satpayev str., 22, 050013, Almaty, Kazakhstan; e-mail: ayazbayeva.aigerim@gmail.com; https://orcid.org/0000-0003-1313-895X;

Nauryzova, Saule Zinagiyevna — PhD, Satbayev University, Satpayev str., 22, 050013, Almaty, Kazakhstan; e-mail: s.nauryzova@satbayev.university; https://orcid.org/0000-0002-3012-7817;

Aseyev, Vladimir Olegovich — PhD, docent, university lecturer, Department of Chemistry, University of Helsinki, P.O. Box 55 (A.I. Virtasen aukio 1), FIN-00014 HY, Helsinki, Finland; e-mail: Vladimir.Aseyev@helsinki.fi; https://orcid.org/0000-0002-3739-8089;

Shakhvorostov, Alexey Valerievich — PhD, Institute of Polymer Materials and Technology, Atyrau-1, 3/1, 050019, Almaty, Kazakhstan; e-mail: alex.hv91@gmail.com; https://orcid.org/0000-0003-3502-6123

*The author's name is presented in the order: *Last Name, First and Middle Names*